Bioorganic & Medicinal Chemistry Letters 22 (2012) 300–304

Contents lists available at SciVerse ScienceDirect

Bioorganic & Medicinal Chemistry Letters

journal homepage: www.elsevier.com/locate/bmcl

3-Heterocyclyl quinolone inhibitors of the HCV NS5B polymerase

Dange V. Kumar [a], Roopa Rai [b,*], Ken A. Brameld [c], Jennifer Riggs [d], John R. Somoza [e], Ravi Rajagopalan [f], James W. Janc [g], Yu M. Xia [h], Tony L. Ton [c], Huiyong Hu [i], Isabelle Lehoux [j], Joseph D. Ho [k], Wendy B. Young [i], Barry Hart [l], Michael J. Green [m]

[a] Myrexis Inc., 305 Chipeta Way, Salt Lake City, UT 84108, USA
[b] Alios BioPharma, 260 E. Grand Ave., South San Francisco, CA 94080, USA
[c] Principia Biopharma, 400 E. Jamie Ct., South San Francisco, CA 94080, USA
[d] Celgene Corp., 4550 Towne Centre Ct., San Diego, CA 92121, USA
[e] Gilead Sciences Inc., 333 Lakeside Drive, Foster City, CA 94404, USA
[f] InterMune Inc., 3280 Bayshore Blvd., Brisbane, CA 94005, USA
[g] Theravance, Inc., South San Francisco, CA 94080, USA
[h] Crown Bioscience, No.6 Beijing West Road, Taicang City, Jiangsu Province 215400, PR China
[i] Genentech Inc., 1 DNA Way, South San Francisco, CA 94080, USA
[j] Allosteros Therapeutics, 1230 Bordeaux Drive, Sunnyvale, CA 94089, USA
[k] Eli Lilly and Company, 10300 Campus Point Drive, Suite 200, San Diego, CA 9212, USA
[l] Innovation Pathways, 20 Palo Alto Ave., Palo Alto, CA 94031, USA
[m] Virobay, Inc., 1490 O'Brien Drive, Menlo Park, CA 94025, USA

ARTICLE INFO

Article history:
Received 13 September 2011
Revised 2 November 2011
Accepted 3 November 2011
Available online 9 November 2011

Keywords:
HCV
NS5B polymerase inhibitors
3-Heterocyclyl quinolone analogs
NNI-2 binders

ABSTRACT

The discovery and optimization of a novel class of quinolone small-molecules that inhibit NS5B polymerase, a key enzyme of the HCV viral life-cycle, is described. Our research led to the replacement of a hydrolytically labile ester functionality with bio-isosteric heterocycles. An X-ray crystal structure of a key analog bound to NS5B facilitated the optimization of this series of compounds to afford increased activity against the target enzyme and in the cell-based replicon assay system.

© 2011 Elsevier Ltd. All rights reserved.

Hepatitis C virus (HCV) infection is a major public health problem with an estimated 170 million patients worldwide.[1] Compromised liver function caused by chronic HCV infection can progress to cirrhosis and hepatocellular carcinoma and is a leading cause for liver transplants.[2] Until recently, HCV therapy consisted of a combination of peginterferon alfa-2a/b and ribavirin, a regimen that has severe limitations including non-response, relapse, poor tolerability and long duration of treatment. Two new small molecule inhibitors of NS3 protease, telaprevir and boceprevir, have completed human clinical trials and been approved for treatment of HCV.[3] Developing novel small molecule inhibitors targeting additional aspects of the HCV life cycle is an active area of research. Both nucleoside and non-nucleoside inhibitors targeting NS5B polymerase are currently in Phase II clinical trials. It is anticipated that NS5B polymerase inhibitors will be used together with NS3 protease inhibitors as the field moves ultimately to combination, all oral therapy for HCV.

Our research led to the discovery of a quinolone-based series of lead compounds which inhibit HCV NS5B polymerase.[4a] The optimization of this new structural class of inhibitors was aided by an X-ray crystallographic structure of the quinolone **1** bound to the NNI-2 allosteric binding site of this enzyme. We now describe efforts to optimize this lead, with the initial goal of replacing the ester functionality with a hydrolytically stable bio-isostere[5] (Fig. 1) to improve activity and metabolic stability. Additionally, we describe substitution on the phenyl rings and at the C7 position of the quinolone to improve the pharmaceutical properties of the series.[6]

Analysis of the X-ray structure of **1** bound to NS5b reveals that the carbonyl of the ester acts as a hydrogen bond acceptor for the backbone NH of Ser 476 in the NNI-2 binding site. An appropriate iso-steric heterocycle should position an H-bond acceptor heteroatom in a similar position. The X-ray structure also reveals that the aromatic ring of the benzyl ester fits into a hydrophobic pocket

* Corresponding author.
E-mail address: roopa.rai@hotmail.com (R. Rai).

0960-894X/$ - see front matter © 2011 Elsevier Ltd. All rights reserved.
doi:10.1016/j.bmcl.2011.11.013

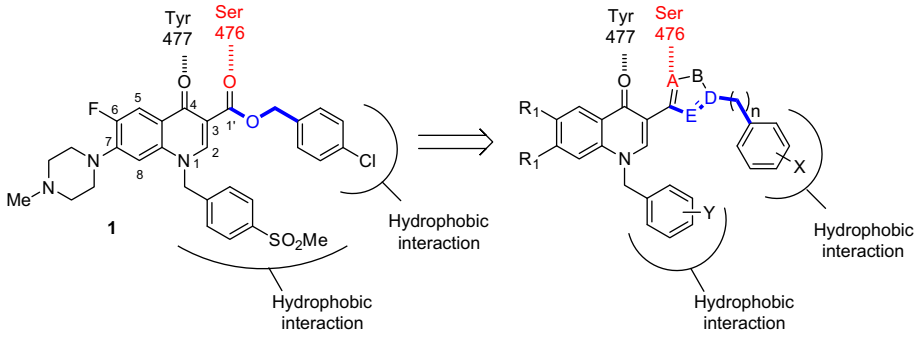

Figure 1. Isosteric replacement of ester with heterocyclic groups.

and is two atoms away from the carbonyl carbon (C1′). We therefore initially prepared the heterocycles **2, 3**, and **4** (Table 1) that possess an H-bond acceptor that corresponds to the position of the ester carbonyl, and a phenyl ring two ($n = 0$) atoms away. The syntheses of these heterocycles are described in Schemes 1–3.[7] Oxadiazoles **2** and **3** are both inactive against NS5B polymerase,[8] whereas the oxazoline **4** displayed some activity but was still much less potent than its ester analog. A reasonable explanation for the observed SAR is apparent from the crystal structure of **1**, where there is a 90° angle between the plane of the ester and the phenyl ring, allowing the ring to be deeply buried in a hydrophobic pocket. Direct substitution from the heteroaromatic rings of **2** and **3** does not allow the phenyl to reach deeply into this out-of-plane hydrophobic pocket. The sp3 linker from the oxazoline ring of **4**, on the other hand, allows the required out-of-plane geometry for the phenyl group to better access the pocket (Fig. 2). Based on this hypothesis, we prepared compounds **5–10** (Schemes 1–3) with a methylene group inserted between the heterocycle and the phenyl group to allow the phenyl group improved access to this hydrophobic pocket.

Our binding hypothesis was supported by the fact that the 1,2,4-oxadiazole **5** was almost equipotent to the ester analog **1**. Compound **10**, with the phenyl group two atoms away from the

Table 1
SAR of C-3 heterocyclic quinolones

#	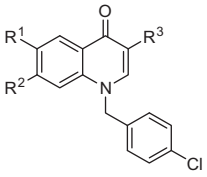			IC_{50}[8] (μM)	EC_{50}[9] (μM)	GI_{50}[9] (μM)
	R^1	R^2	R^3			
2	OCH_3	OCH_3		>10	–	–
3	OCH_3	OCH_3	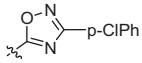	>10	–	–
4	OCH_3	OCH_3		4.3	8.91	–
5	OCH_3	OCH_3	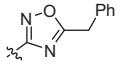	0.041	10.3	–
6	OCH_3	OCH_3	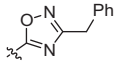	0.73	–	–
7	OCH_3	OCH_3	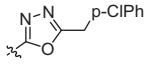	1.6	–	–
8	OCH_3	H	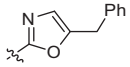	1.8	–	–
9	OCH_3	OCH_3	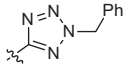	>10	–	–
10	OCH_3	OCH_3	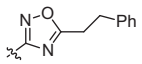	>10	–	–
11	F		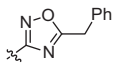	0.023	0.84	7.3
12	F		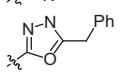	0.115	4.4	9.8

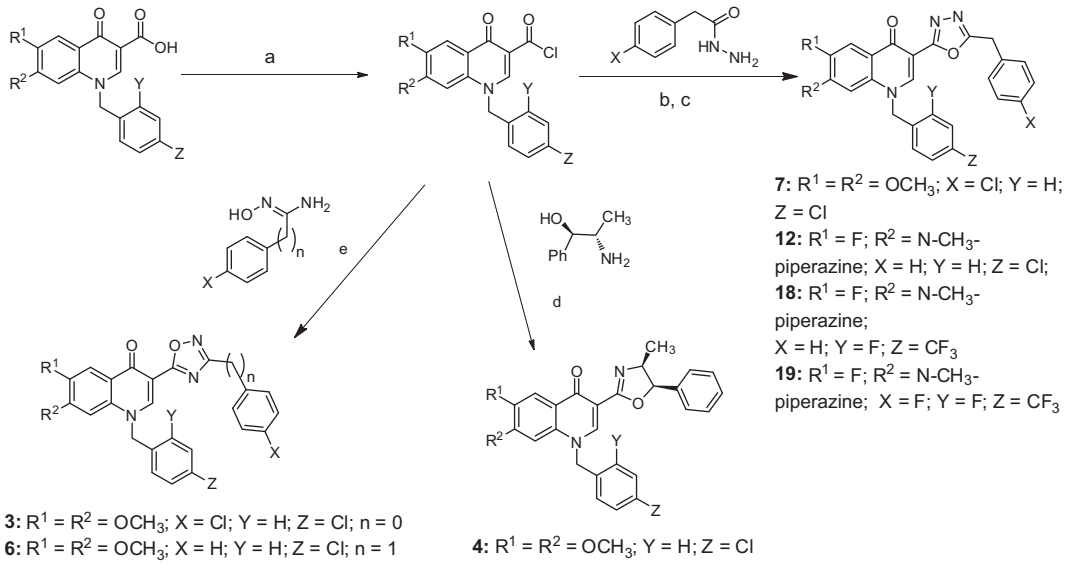

Scheme 1. Reagents and conditions: (a) Polystyrene bound-PPh_3 (PS-PPh_3), Cl_3CCN, THF, 100 °C, 10 min; (b) DIEA, 150 °C or microwave, 15 min; (c) PS-PPh_3, I_2, TEA, DCM, 0 °C to rt; (d) Et_3N; (e) K_2CO_3.

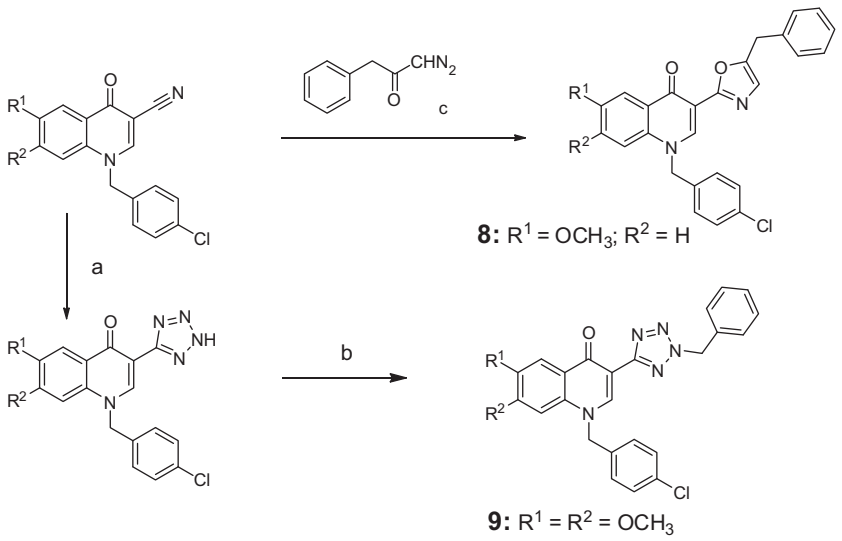

Scheme 2. Reagents and conditions: (a) $TMSN_3$, *n*-Bu2SnO, toluene, 110 °C, 4 h; (b) Benzyl bromide, K_2CO_3, DMF, 60 °CC, 4 h; (c) $BF_3{\cdot}OEt2$, CH_2Cl_2.

heterocyclic ring, was devoid of NS5b polymerase inhibitory activity. The isomeric 1,2,4-oxadiazole **6** was also active but 20-fold less potent than **5**, indicating that the oxygen is less capable of forming the required H-bond than the nitrogen in **5**. The 1,3,4-oxadiazole **7** and the oxazole **8** were even less potent while the tetrazole **9** was inactive.

Despite being a potent inhibitor of the NS5B enzyme, the oxadiazole **5** was poorly active in the replicon assay.[9] In parallel, compounds were evaluated for their cytotoxic effects in the replicon cell line.[9] To improve the replicon activity, we turned our attention to improving the biopharmaceutical properties of this class of compounds. The X-ray structure of ester **1** indicates that substituents at the C7 position point into bulk solvent and positioning hydrophilic substituents at this site led to good replicon potency in the ester series.[4] We applied the same strategy to the oxadiazole heterocycles **5** and **7**. The 6-fluoro-7-(*N*-methylpiperizine)-analogs of these compounds, **11** and **12**, were synthesized according to Schemes 1 and 3. Compounds **11** and **12** did indeed have improved replicon potency.[4b] In particular, the submicromolar replicon potency of **11** encouraged us to continue optimizing this series.

The two phenyl rings were modified with electron withdrawing substitutents to optimize potency and block potential phenyl ring oxidative metabolism.[7] The results of this work are shown in Tables 2 and 3. In the 1,2,4-oxadiazole series, replacing the R4 phenyl ring with a 4-F-phenyl (**13**, Table 2) results in no loss of activity against NS5B, while replacing it with a 2,4-difluoro phenyl ring (**14**) reduces both NS5B and replicon potency. Replacing the p-chlorine on the *N*-benzyl group of **11** (Table 2) with 4-trifluoromethyl (**15**) or with 2-fluoro-4-trifluoromethyl (**16**) maintained the potency against NS5B and further improved replicon potency. Compound **17**, which has both phenyl rings protected from metabolic oxidation, was highly potent in both assays. These substitutions also improved replicon potency in the 1,3,4-oxadiazole series, compounds **18** and **19** in Table 3.[10]

In order to confirm our design paradigm and to guide further optimization, the structure of **16** bound to NS5B was solved (RCSB

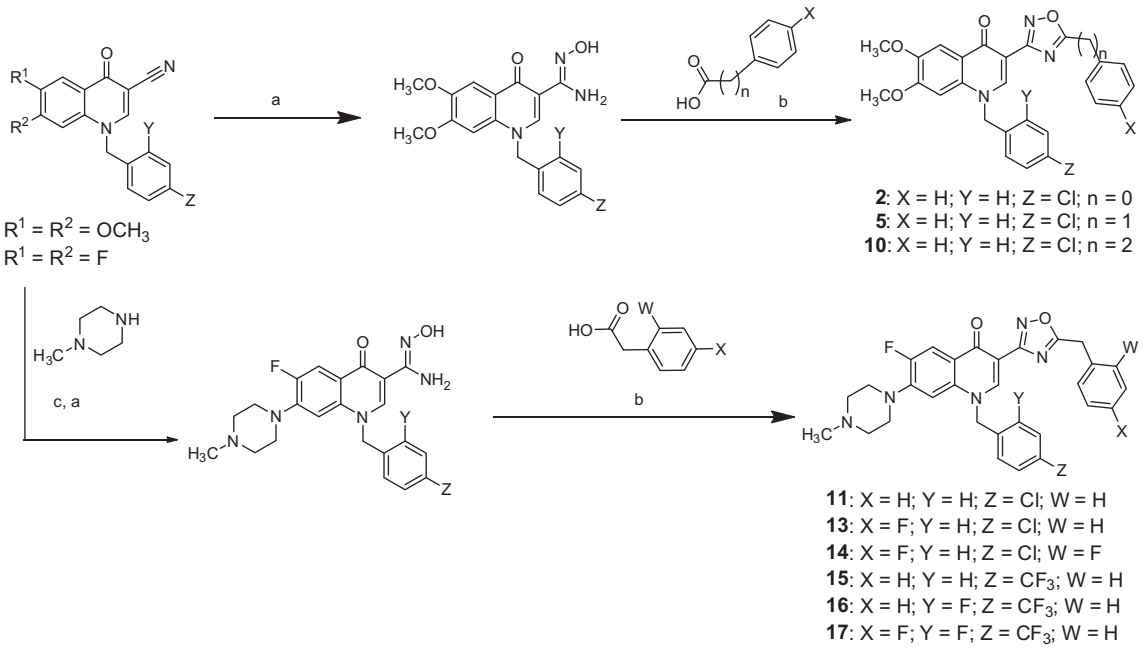

Scheme 3. Reagents and conditions: (a) NH_2OH, DIEA, aq EtOH; (b)HBTU, DIPEA, 200 °C, microwave; 3 min (c) acetonitile, reflux.

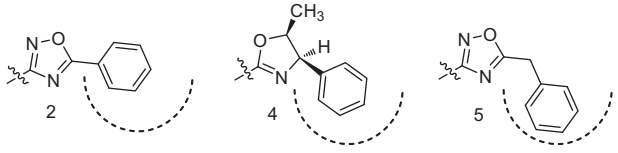

Figure 2. Design optimization for best fit of phenyl ring in hydrophobic pocket.

Table 2
Optimization of the 3-(1,2,4-oxadiazole)-quinolone series

#	R^3	R^4	IC_{50} (μM)	EC_{50} (μM)	GI_{50} (μM)
13	4-FPh	4-ClPh	0.019	1.43	6.4
14	2,4-DiFPh	4-ClPh	0.075	3.68	4.7
15	Ph	4-CF_3Ph	0.024	0.36	15
16	Ph	2-F, 4-CF_3Ph	0.014	0.25	7.0
17	4-FPh	2-F, 4-CF_3Ph	0.015	0.23	6.0

Table 3
Optimization of the 3-(1,3,4-oxadiazole)-quinolone series

#	R^3	R^4	IC_{50} (μM)	EC_{50} (μM)	GI_{50} (μM)
18	Ph	2-F,4-CF_3Ph	0.038	0.61	4.6
19	p-FPh	2-F,4-CF_3Ph	0.045	0.73	5.7

ID code: RCSB068620; PDB ID code: 3UDL). The construct of NS5B had the N-terminal 21 residues removed and included a His tag at the C-terminus. The structure was refined to 2.15 Å resolution (R = 0.191, FreeR = 0.243, RMS bonds = 0.03 Å, RMS angles = 0.69°). Generally, each of the four molecules in the asymmetric unit showed clear electron density for the inhibitor, although the density for the N-methyl piperazine, which points into solution was less well defined. The crystal structure revealed a binding mode consistent with that observed for compound **1**. The ligand occupies the NNI-2 binding site located in the thumb region (Fig. 3a), making several hydrogen bonds and occupying two hydrophobic pockets. The quinolone ring sits on a shelf formed by Ile 482. As expected, a hydrogen bond exists between the quinolone carbonyl oxygen atom and the backbone amide NH of Tyr 477. In addition, the N2 nitrogen atom of the oxadiazole is nicely positioned to receive a hydrogen bond from the backbone amide NH of Ser 476. The benzyl group off the oxadiazole occupies a hydrophobic pocket formed by the collapse of Leu 419, Arg 422, Met 423, and Trp 528. A second shallow hydrophobic pocket is occupied by the CF_3-phenyl group which contacts Leu 419, Val 485, Ala 486, Leu 489, Leu 497, and Met 423. Finally, the piperazine ring is solvent exposed, consistent with the suitability of this location for modulating the overall physico-chemical properties of the molecule.

An overlay of the X-ray structures for compounds **1** and **16** (Fig. 3b) confirms the design hypothesis used to drive the replacement of the benzyl ester with a benzyl oxadiazole. The methylene linker of the benzyl group allows the phenyl ring to adopt the preferred out-of-plane geometry and the two rings are nearly superimposable, despite the longer overall linker length of the oxadiazole when compared to the ester. The CF_3 group at the phenyl R4 position overlays well with the methylsulfone of **1**, although the benzyl rings are twisted approximately 45° relative to each other.

The origin of this rotational difference is not readily apparent. The ortho-fluoro substituent on the *N*-benzyl ring of **16** does not make any specific interactions with the proximal residues of the binding pocket. Thus the twist is likely a consequence of either an intramolecular interaction between the *ortho*-fluoro and methylene of the benzyl group or the influence of the methyl sulfone on the phenyl ring of **1**. In the absence of additional structural data, it

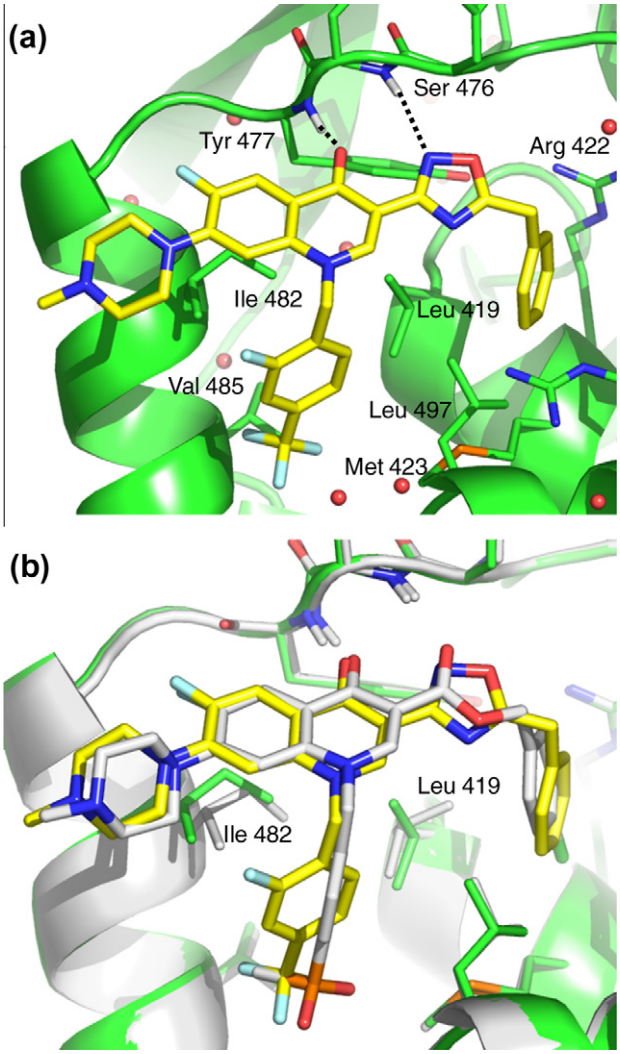

Figure 3. (a) X-ray structure of **16** bound to NNI-2 site (PDB ID code: 3UDL). (b) Overlay of compounds **16** (yellow) and **1** (white), showing a high degree of overlap between the two ligands and very similar protein conformations. Small differences in Leu 419 and Ile 482 are highlighted.

is difficult to assess the validity of either of these hypotheses. However, this observation suggests that the interactions made by the aromatic portion of the benzyl substituent in this region of the binding pocket are weak, non-specific, and easily influenced by subtle chemical changes.

Scheme 1 describes the conversion of a C3 carboxylic acid to various ester isosteric heterocycles. Activation of the acid as the acid chloride affords an intermediate that reacts with a hydroxamidine, 1,2-amino alcohol or hydrazide to afford a 1,2,4-oxadiazole (**3, 6**), 1,3-oxazoline (**4**), and a 1,3,4 oxadiazole respectively (**7, 8, 12, 19**). Scheme 2 describes the conversion of the C3 quinolone nitrile to the C3 oxazole and tetrazole derivatives. Reaction of the nitrile with $TMSN_3$ affords the intermediate tetrazole that is benzylated to afford compound **9**.[11] Oxazole **8** is obtained by reacting the nitrile with 1-diazo-3-phenylpropan-2-one.

Scheme 3 describes the conversion of quinolone C3 nitriles to the intermediate hydroxyamidine through reaction with hydroxyl amine. The resulting hydroxyamidine intermediates are converted to a variety of 1,2,4-oxadiazole target compounds by reacting with appropriate carboxylic acids.

In conclusion, we have described a new series of allosteric-site (NNI-2) inhibitors of the HCV NS5B polymerase enzyme. These compounds are an improvement on a previous series of quinolones through the replacement of an ester with either a 1,2,4- or a 1,3,4-oxadiazole. The most potent compounds in this series, **16** and **17**, have replicon EC_{50}s below 250 nM. The continued optimization of this series will be described in forthcoming papers.

Acknowledgement

The authors thank Dr. Robert Booth (Virobay Inc.) for support of the research that went into this paper.

References and notes

1. Simmonds, P. *J. Gen. Virol.* **2004**, *85*, 3173.
2. Younossi, Z.; Kallman, J.; Kincaid, J. *Hepatology* **2007**, *45*, 806.
3. (a) Poordad, F.; McCone, J.; Bacon, B. R.; Bruno, S.; Manns, M. P.; Sulkowski, M. S.; Jacobson, I. M.; Reddy, K. R.; Goodman, Z. D.; Boparai, N.; DiNubile, M. J.; Sniukiene, V.; Brass, C. A.; Albrecht, J. K.; Bronowicki, J. P. N. SPRINT-2 Investigators *Engl. J. Med.* **2011**, *364*, 1195; (b) Jacobson, I. M.; McHutchison, J. G.; Dusheiko, G.; Di Bisceglie, A. M.; Reddy, K. R.; Bzowej, N. H.; Marcellin, P.; Muir, A. J.; Ferenci, P.; Flisiak, R.; George, J.; Rizzetto, M.; Shouval, D.; Sola, R.; Terg, R. A.; Yoshida, E. M.; Adda, N.; Bengtsson, L.; Sankoh, A. J.; Kieffer, T. L.; George, S.; Kauffman, R. S.; Zeuzem, S. N. ADVANCE Study Team *Engl. J. Med.* **2011**, *364*, 2405.
4. (a) Kumar, D. V.; Rai, R.; Brameld, K. A.; Somoza, J. R.; Rajagopalan, R.; Janc, J. W.; Xia, Y. M.; Ton, T. L.; Shaghafi, M. B.; Hu, H.; Lehoux, I.; To, N.; Young, W. B.; Green, M. J. *Bioorg Med Chem Lett* **2011**, *21*, 82; (b) While protein binding and solubility of the lead ester series was not evaluated, the improvement in replicon potency with the addition of polar moieties at the C7 position is attributed to reduced protein binding properties.
5. (a) Saunders, J.; Angus, M.; MacLeod, K. M.; Showell, G. A.; Snow, R. J.; Street, L. J.; Baker, R. *J. Chem. Soc., Chem. Commun.* **1988**, 1618; (b) Kuduk, S. D.; Chang, R. K.; Ng, C.; Murphy, K. L.; Ransom, R. W.; Tang, C.; Prueksaritanont, T.; Freidinger, R. M.; Pettibone, D. J.; Bock, M. G. *Bioorg. Med. Chem. Lett.* **2005**, *15*, 3925.
6. Smith, D. A.; Waterbeemd, H.; Walker, D. K. In *Pharmacokinetics and Metabolism in Drug Design*; Mannhold, R., Kubinyi, H., Folkers, G., Eds.; Wiley-VCH: Weinheim, Germany, 2006. second Ed., Vol. 31.
7. Kumar, D. V.; Rai, R.; Young, W. B.; Hu, H, Riggs, J. R.; Ton, T. L.; Green, M. J.; Hart, B. P.; Brameld, K. A.; Dener, J. M. US 2007/0287699 and WO 2007/130499.
8. The NS5B polymerase IC50 enzyme activity assay determination: As described in: McKercher, G.; Beaulieu, P. L.; Lamarre, D.; LaPlante, S.; Lefebvre, S.; Pellerin, C.; Thauvette, L.; Kukolj, G. Nuc. Acids Res. 2004, 32, 422. Scintillation proximity assays (SPA) were performed at ambient temperature (22 °C) in 96-well plates using 50 nM of enzyme (a C-terminal 21 residue deletion mutant of NS5b from genotype 1b BK isolate). Reaction components included 20 mM Tris–HCl pH 7.5, 5 mM MgCl2, 1 mM EDTA, 2 mM DTT, 5% DMSO, 0.01% BSA and 25 mM KCl. 80 μl reactions were initiated by adding a mixture of 0.5 μCi of [3H]UTP, 1 μM UTP, 250 nM 5′-biotinylated oligo(rU12) and 0.8 μg/ml poly(rA) to assay wells containing enzyme preincubated with inhibitor. Reactions were terminated after 120 min by the addition of 20 μl of stop solution containing 150 μg/ml tRNA and 10 mg/ml streptavidin-coated SPA beads (Amersham) in 20 mM Tris–HCl pH 7.5, 25 mM KCl, 0.5 M EDTA and 0.025% sodium azide. After incubation for 30 min, 65 μl of 5 M cesium chloride were added to the wells and further incubated for 1 h before top-counting in a Microbeta Trilux plate reader.
9. The cell-based Replicon EC_{50} determination: HCV replicon-containing cells (Huh7/Clone A, genotype 1b) were maintained in growth medium (DMEM medium, Invitrogen), supplemented with 10% Fetal Bovine Serum, non essential amino acids and 1 mg/mL G418) (Blight K. J., Kolykhalov A. A. and Rice C. M. (2000) Science 290, 1972–1974). For the HCV replicon assay, Huh7/Clone A cells were trypsinized from culture flasks, seeded in 1 ml of Clone A growth medium without G418 at 40,000 cells per well in 24-well plates and incubated at 37 °C in a humidified CO2 (5%) incubator overnight. Following overnight incubation, test compound was serially diluted in DMSO and added to the test system such that the final concentration of DMSO was 0.5% in each well. For IC50 determinations, compounds were tested at 7 concentrations in triplicates. Plates were incubated at 37 °C for 48 h. After incubation, cells were harvested, transferred to 96-well plates, and subjected to total RNA extraction using the RNA Isolation Kit (RNeasy 96, Qiagen). TaqMan quantitative PCR (RT-qPCR) was used to quantify the amount of HCV replicon RNA in each sample. The samples without compound treatment served as a control and the HCV replicon RNA level from untreated cells was defined as 100%. Compound inhibitory activity was determined as the ratio of the normalized HCV RNA amount in treated samples relative to the untreated control. Compound EC50's were calculated using a standard 4 parameter curve fit model. The cytotoxicity of compounds, the GI_{50},was assayed in parallel in which qPCR of the cellular host protein GAPDH was used as an indicator of viable cells.
10. In general, the 7-position piperazine substituted compounds had low stability in human liver microsomes with 20–50% remaining after a 1 h incubation.